

## Cytotoxic Evaluation and Lichenochemical Characterization of *Diploschistes ocellatus* with In Silico Survivin Inhibition Analysis

Nour Abdelrahman<sup>1\*</sup>, Ahmed El-Kholy<sup>1</sup>, Karim Hassan<sup>2</sup>

<sup>1</sup>Department of Pharmacognosy, Faculty of Pharmacy, Mansoura University, Mansoura, Egypt.

<sup>2</sup>Department of Biotechnology, Faculty of Science, Suez Canal University, Ismailia, Egypt.

\*E-mail ✉ [nour.abdelrahman@outlook.com](mailto:nour.abdelrahman@outlook.com)

Received: 14 October 2024; Revised: 14 January 2025; Accepted: 18 January 2025

### ABSTRACT

*Diploschistes ocellatus* (Fr.) Norman is a medicinally important lichen with reported biological activities and a history of traditional use by indigenous populations in southwestern Iran for treating various ailments. The present study aimed to assess the cytotoxic effects of different solvent fractions of *D. ocellatus* on breast cancer cell lines using the MTT assay, to perform lichenochemical characterization of the most active fraction, and to investigate interactions between isolated compounds and target proteins through molecular docking analysis. Aqueous, acetone, chloroform, ethyl acetate, and methanolic fractions of *D. ocellatus* were prepared and evaluated for cytotoxic activity against three human breast cancer cell lines (MCF-7, T-47D, and MDA-MB-231) using the MTT method. Molecular docking studies were conducted employing AutoDock 4.2 software with standard protocols and default parameters. Among the tested fractions, the acetone extract exhibited the strongest cytotoxic activity and was therefore selected for further phytochemical investigation. Lichenochemical analysis of this fraction resulted in the isolation and identification of stictic acid and 2-(7'-hydroxy-3,5,6,8-tetramethyl-9-oxooxonan-2-yl) propanoic acid. Molecular docking simulations targeting survivin demonstrated favorable binding interactions between the isolated compounds and key amino acid residues of the protein. The findings suggest that *D. ocellatus* represents a promising natural source of bioactive compounds with potential anticancer properties. Further pharmacological and mechanistic studies are warranted to validate and expand upon these results.

**Keywords:** *Diploschistes ocellatus*, Lichens, Isolation, Breast cancer, Molecular docking simulation

**How to Cite This Article:** Abdelrahman N, El-Kholy A, Hassan K. Cytotoxic Evaluation and Lichenochemical Characterization of *Diploschistes ocellatus* with In Silico Survivin Inhibition Analysis. *Spec J Pharmacogn Phytochem Biotechnol.* 2025;5:235-42. <https://doi.org/10.51847/qWp7iFN9m2>

### Introduction

Lichens are complex symbiotic organisms formed through the association of fungi with algae or cyanobacteria. They inhabit diverse substrates, including tree bark, rocks, walls, and soil, and are widely distributed across various ecosystems worldwide [1]. Secondary metabolites produced by lichens exhibit a broad spectrum of biological activities, such as enzyme inhibition, antioxidant, antifungal, antimicrobial, anticancer, antiviral, and insecticidal effects [2]. In Persian traditional medicine, lichens are referred to as “hazaz-al-sakhr” and have historically been used for medicinal purposes, including wound healing and the treatment of bleeding disorders and skin conditions such as eczema and inflammation [3].

Lichens synthesize a diverse array of bioactive compounds, including sugar alcohols, amino acid derivatives, aliphatic acids, quinones, macrolide lactones, monocyclic aromatic compounds, xanthenes, chromones, depsides, dibenzofurans, depsidones, terpenoids, depsones, carotenoids, steroids, and diphenyl ethers, many of which possess significant biological activities [4]. Among these compounds, usnic acid (2,6-diacetyl-7,9-dihydroxy-8,9b-dimethyl-1,3(2H,9bH)-dibenzofurandione) and its semisynthetic derivatives have attracted considerable

attention due to their notable pharmacological properties, particularly their anticancer potential [5]. In addition, numerous studies have confirmed the strong cytotoxic activities of depsides and depsidones [6].

*Diploschistes* (family Thelotremaaceae) is a genus of crustose lichens comprising approximately 43 species that predominantly grow in arid and semi-arid regions worldwide. Among these species, *Diploschistes ocellatus* (Fr.) Norman (synonym: *Xalocoa ocellata* (Fr.) Kraichak, Lücking & Lumbsch) has been traditionally utilized by indigenous communities in southwestern Iran. Previous studies have reported the antimicrobial and antioxidant properties of *D. ocellatus* [7, 8]. Furthermore, Mendili *et al.* demonstrated notable DPPH radical-scavenging and iron-chelating activities of the methanolic fraction of *D. ocellatus*, while the acetone extract exhibited the highest ferric-reducing antioxidant power [8].

Despite extensive advances in cancer treatment, therapeutic efficacy remains limited by the development of drug resistance, often involving resistance to multiple chemotherapeutic agents, a phenomenon known as multidrug resistance (MDR). Chemotherapy primarily exerts its anticancer effects by triggering apoptosis, a programmed cell death process mediated through multiple signaling pathways. Apoptotic regulation involves a balance between pro-apoptotic and anti-apoptotic proteins, including members of the inhibitors of apoptosis (IAPs) and B-cell lymphoma-2 (Bcl-2) families. Disruption of apoptotic pathways is recognized as a major contributor to MDR [9]. Caspases, a family of cysteine-dependent aspartate-specific proteases, play essential roles in the execution of apoptosis. These enzymes are synthesized as inactive pro-enzymes containing an N-terminal pro-domain and a C-terminal catalytic domain. Human caspases are classified into initiator caspases (caspase-2, -8, -9, and -10) and effector caspases (caspase-3, -6, and -7). The ultimate fate of a cell is determined by the intricate crosstalk between pro-apoptotic and anti-apoptotic signaling mechanisms. Survivin, the smallest member of the IAP family, directly suppresses the activity of caspases-3 and -7 through its baculoviral IAP repeat (BIR) domain, thereby inhibiting protease activity and preventing downstream apoptotic events [10, 11]. Owing to its selective overexpression in cancer cells, survivin is considered a cancer-specific biomarker and an important molecular target in anticancer therapy, with survivin inhibitors gaining increasing attention in drug development [12].

To the best of our knowledge, the cytotoxic potential of *D. ocellatus* has not been previously investigated. Therefore, the present study aimed to evaluate the cytotoxic effects of different solvent fractions of *D. ocellatus* against three human breast cancer cell lines (T-47D, MCF-7, and MDA-MB-231). In addition, lichenochemical analysis was performed on the most active fraction, and molecular docking studies were conducted to assess the potential involvement of the isolated compounds in survivin inhibition.

## Materials and Methods

### *Ethical approval*

Approval for conducting this research was obtained from the Institute of Pharmaceutical Sciences, Tehran University of Medical Sciences. The study was carried out in accordance with institutional guidelines and assigned the ethical approval code IR.TUMS.TIPS.REC.1401.107.

### *Reagents and materials*

Analytical-grade solvents and reagents were used throughout the study. Chromatographic separations were performed using silica gel of varying mesh sizes (Merck, Germany), aluminum-backed TLC plates (Si gel 60 F254 and RP-18 F254; Merck, Germany), Sephadex LH-20, and RP-18 materials (Fluka, Switzerland). For cell culture and cytotoxicity assays, RPMI 1640 medium (PAA, Germany), N-hydroxyethylpiperazine-N-2-ethanesulfonic acid (HEPES; Biosera, England), fetal bovine serum (FBS; Gibco, USA), and the tetrazolium salt MTT (3-[4,5-dimethylthiazol-2-yl]-2,5-diphenyltetrazolium bromide; Sigma-Aldrich, USA) were employed.

### *Lichen sampling and identification*

Specimens of the lichen were harvested in October 2017 from Kohgiluyeh va Boyer Ahmad Province in southwestern Iran. Species identification was carried out by Dr. Mohammad Sohrabi, an expert lichenologist. A voucher specimen was deposited at the ICH Lichen Herbarium of the Iranian Research Organization for Science and Technology with accession number ICH 16670.

### *Extraction and fractionation procedure*

After collection, the lichen material was carefully washed, air-dried under ambient conditions, and ground into powder. The dried powder (700 g) was separated into two equal portions. The first portion (350 g) underwent sequential extraction by maceration using chloroform, ethyl acetate, and methanol. The second portion (350 g) was extracted in a similar manner using acetone followed by distilled water. Each extract was filtered, concentrated under reduced pressure, and allowed to dry completely. The obtained residues were preserved at low temperature until subsequent experiments were performed [13].

#### *Cell culture and cytotoxicity assessment*

Human breast carcinoma cell lines MCF-7, MDA-MB-231, and T-47D were supplied by the Pasteur Institute of Iran (Tehran, Iran). Cells were maintained in RPMI 1640 culture medium supplemented with sodium bicarbonate, HEPES buffer, fetal bovine serum, penicillin (100 U/mL), and streptomycin (100 µg/mL). Incubation was conducted at 37 °C in a humidified atmosphere containing 5% CO<sub>2</sub>. The cytotoxic potential of different *D. ocellatus* fractions was determined using the MTT colorimetric assay based on the reduction of 3-[4,5-dimethylthiazol-2-yl]-2,5-diphenyltetrazolium bromide, following the previously established protocol [14].

#### *Purification and isolation of compounds*

The acetone extract (3 g) was fractionated using silica gel column chromatography (30–70 mesh, 3 × 45 cm). Elution was carried out with a stepwise solvent gradient starting from chloroform/acetone (10:0 gradually to 0:10), followed by acetone/methanol (10:0 gradually to 0:10), yielding ten primary fractions (AC1–AC10). Fraction AC6 (110 mg) was further purified by chromatography on a Sephadex LH-20 column (2 × 60 cm) using methanol as the mobile phase, resulting in six subfractions (AC6a–AC6f). Subfraction AC6c afforded compound A after recrystallization with *n*-hexane. Subsequently, fraction AC6f was subjected to an additional Sephadex LH-20 chromatographic separation (2 × 60 cm) with methanol elution, producing five subfractions (AC6f1–AC6f5). Among these, AC6f2 was obtained as compound B [15].

#### *Docking study*

Molecular docking analysis was carried out to explore the interaction between the isolated ligands and target proteins using AutoDock 4.2 software with standard settings and the conventional docking protocol [16]. The anti-apoptotic protein survivin was selected as the molecular target due to its role in apoptosis regulation. Docking procedures were performed in accordance with previously reported methodologies [17, 18]. The amino acid sequence of human survivin was retrieved from the NCBI database ([www.ncbi.nlm.nih.gov](http://www.ncbi.nlm.nih.gov)), and its three-dimensional crystallographic structure was obtained from the RCSB Protein Data Bank (<http://www.rcsb.org>). Survivin exists as a homodimer composed of A and B chains, which share nearly identical sequences, with chain B differing only by the presence of two additional C-terminal residues (Met and Asp). For docking simulations, chain A was selected as the receptor model [19].

Two-dimensional chemical structures of the isolated compounds were drawn using ChemOffice 2015 and subsequently subjected to energy minimization with HyperChem 7.0 software (Hypercube Inc., Gainesville, FL, USA; <http://www.hyper.com>). The optimization parameters followed protocols previously described in the literature [17, 18]. The ligand-binding site on survivin was defined based on data from site-directed mutagenesis studies. Accordingly, a grid box was centered on the survivin structure (PDB ID: 1E31) with a resolution of 2.71 Å [20], using coordinates X = -24.532, Y = 36.317, and Z = 64.94 [21]. Grid maps were generated using AutoGrid 4 with dimensions of 60 × 60 × 60 points along the x, y, and z axes and a grid spacing of 0.375 Å. Docking results were clustered after completion of 200 docking runs [18]. The Lamarckian Genetic Algorithm (LGA) implemented in AutoDock was employed to predict the most favorable ligand conformations and binding modes [22].

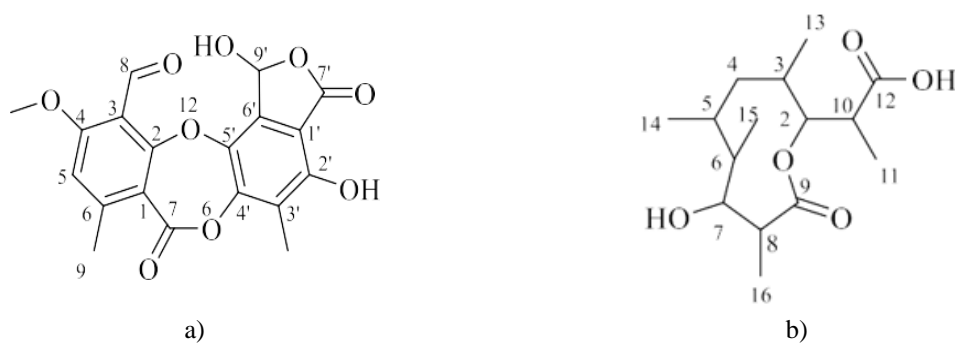


**Figure 1.** Molecular structures of compounds a (stictic acid) and b (2-(7'-hydroxy-3,5,6,8-tetramethyl-9-oxooxonan-2-yl)propanoic acid) isolated from *Diploschistes ocellatus*.

Docking scores and binding energies were computed using AutoDock 4.2. From the ensemble of ligand–survivin binding conformations generated during the docking simulations, the pose exhibiting the minimum binding energy and the most stable interaction profile was selected for further analysis (**Table 1**). To facilitate interpretation of ligand–protein interactions, the selected complexes were converted into two-dimensional interaction diagrams and examined graphically using LigPlot software [23].

#### Statistical analysis

Statistical evaluation was conducted using Microsoft Excel 2010. Experimental results are reported as mean  $\pm$  standard deviation (SD), calculated from three independent replicates.

### Results and Discussion

Structural elucidation of the metabolites isolated from *D. ocellatus* (designated compounds A and B) was accomplished through detailed nuclear magnetic resonance (NMR) spectroscopic analyses, and the identified structures are presented in **Figure 1**.

Compound A was isolated as white crystalline material (10 mg). Comparative analysis of its spectroscopic data with previously published reports confirmed its identity as stictic acid [24].

$^1\text{H}$  NMR (500 MHz,  $\text{DMSO-d}_6$ ):  $\delta$  10.43 (1H, s, CHO-8), 7.09 (1H, s, H-5), 6.86 (1H, s, H-9'), 3.84 (3H, s, OMe-4), 2.46 (3H, s, Me-9), 2.20 (3H, s, Me-8').

$^{13}\text{C}$  NMR (125 MHz,  $\text{DMSO-d}_6$ ):  $\delta$  194.4 (C-8), 166.6 (C-2), 163.0 (C-7'), 162.0 (C-4), 161.45 (C-7), 155.0 (C-2'), 153.5 (C-6), 143.8 (C-4'), 142.8 (C-5'), 142.0 (C-6'), 117.8 (C-3'), 112.0 (C-3), 111.3 (C-1), 111.0 (C-5), 108.6 (C-1'), 95.8 (C-9'), 56.7 (C-4-OMe), 22.1 (C-9), 10.1 (C-8').

Compound B was obtained as a white amorphous powder and produced a dark blue coloration following treatment with *p*-anisaldehyde–sulfuric acid reagent and subsequent heating. Its molecular formula was established as  $\text{C}_{15}\text{H}_{26}\text{O}_5$  based on electron impact mass spectrometry, which showed a molecular ion peak at  $m/z$  286.6  $[\text{M}]^+$  (calculated 286.18), corresponding to three degrees of unsaturation. Analysis of the  $^{13}\text{C}$  NMR spectrum revealed 15 distinct carbon signals. DEPT and HSQC experiments enabled classification of these carbons as five methyl groups, one methylene carbon, seven methine carbons, and two carbonyl carbons. The  $^1\text{H}$  NMR spectrum exhibited characteristic resonances attributable to four methyl doublets ( $\delta_{\text{H}}$  0.86, 0.89, 1.08, and 1.16), a methyl broad singlet at  $\delta_{\text{H}}$  0.84, and an oxygen-bearing methine proton at  $\delta_{\text{H}}$  3.72 (dd,  $J = 9.5$  and 2.1 Hz). Definitive proton assignments and structural connectivity were confirmed through comprehensive interpretation of  $^1\text{H}$ – $^1\text{H}$  COSY, HSQC, and HMBC correlation spectra (**Figure 2**).

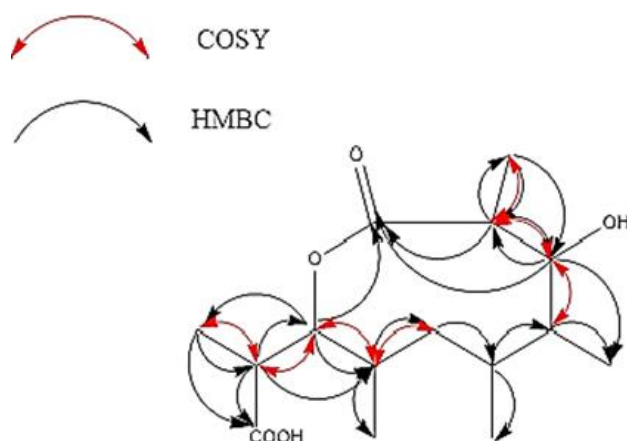


**Figure 2.** Diagnostic  $^1\text{H}$ – $^1\text{H}$  COSY correlations (red arrows) together with long-range  $^1\text{H}$ – $^{13}\text{C}$  HMBC connectivities (black arrows) observed for compound B.

Interpretation of the combined 1D and 2D NMR data enabled unambiguous structural determination of compound B as 2-(7'-hydroxy-3,5,6,8-tetramethyl-9-oxooxonan-2-yl)propanoic acid.

$^1\text{H}$ -NMR ( $\text{CDCl}_3$ , 400 MHz):  $\delta$  0.84 (3H, bs, H-15), 0.86 (3H, d,  $J = 2.1$  Hz, H-14), 0.89 (3H, d,  $J = 3.3$  Hz, H-13), 0.9 (1H, bs, H-4 $\alpha$ ), 1.08 (3H, d,  $J = 7.1$  Hz, H-16), 1.16 (3H, d,  $J = 7.2$  Hz, H-11), 1.25 (1H, bs, H-4 $\beta$ ), 1.45 (1H, m, H-5), 1.71 (1H, m, H-6), 1.90 (1H, m, H-3), 2.60 (1H, m, H-8), 2.77 (1H, m, H-10), 3.72 (1H, dd,  $J = 2.1$  Hz, 9.5 Hz, H-7), 5.17 (1H, dd,  $J = 2.1$  Hz, 9.7 Hz, H-2).  $^{13}\text{C}$ -NMR ( $\text{CDCl}_3$ , 100 MHz):  $\delta$  11.1 (C-14), 12.5 (C-15), 13.7 (C-11), 13.8 (C-13), 14.5 (C-16), 30.7 (C-3), 30.8 (C-6), 31.2 (C-5), 41.1 (C-4),

Phylogenetic evaluation of the *Diploschistes* genus has demonstrated that *D. ocellatus* represents a distinct monotypic lineage classified within *Diploschistes* subgenus *Thorstenia*. According to Fernández-Brime *et al.*, a key taxonomic marker separating this species from other members of the genus is the dominance of  $\beta$ -orcinol depsidones rather than orcinol depsides [25, 26]. Consistent with this chemotaxonomic criterion, stictic acid—a representative  $\beta$ -orcinol depsidone—was isolated from the acetone extract of *D. ocellatus* in the current investigation.

Cytotoxic screening of *D. ocellatus* fractions was performed using three human breast carcinoma cell models (MCF-7, T-47D, and MDA-MB-231), with etoposide serving as the reference anticancer agent (**Table 2**). The aqueous extract exhibited no measurable cytotoxic response toward any tested cell line ( $\text{IC}_{50} > 500$   $\mu\text{g}/\text{mL}$ ). In contrast, marked inhibitory activity was detected for both acetone and ethyl acetate fractions. For MCF-7 cells,  $\text{IC}_{50}$  values of 80.87  $\mu\text{g}/\text{mL}$  (acetone) and 81.23  $\mu\text{g}/\text{mL}$  (ethyl acetate) were recorded. A similar trend was observed for T-47D cells, although the acetone fraction demonstrated superior potency ( $\text{IC}_{50} = 81.20$   $\mu\text{g}/\text{mL}$ ) compared to the ethyl acetate extract ( $\text{IC}_{50} = 102.88$   $\mu\text{g}/\text{mL}$ ). Reduced sensitivity was noted in the MDA-MB-231 cell line, where  $\text{IC}_{50}$  values increased to 144.36  $\mu\text{g}/\text{mL}$  and 114.41  $\mu\text{g}/\text{mL}$  for the acetone and ethyl acetate fractions, respectively. Extracts obtained using chloroform and methanol showed only moderate growth inhibition. These comparative results justified selection of the acetone fraction for detailed phytochemical investigation.

Previous studies have documented the anticancer potential of stictic acid [27], including moderate cytotoxicity against HT-29 colon cancer cells ( $\text{IC}_{50} = 29.29$   $\mu\text{g}/\text{mL}$ ) accompanied by minimal toxicity toward normal MRC-5 fibroblasts ( $\text{IC}_{50} = 2478.40$   $\mu\text{g}/\text{mL}$ ) [28]. In contrast, biological data regarding compound B remain scarce, highlighting the necessity for further pharmacological evaluation.

Molecular docking analysis demonstrated that both isolated compounds occupied the survivin binding pocket and interacted with several functionally important residues, namely Phe61, Cys60, Glu63, Lys62, Ser81, His80, Asn111, Gly83, Asn118, Lys115, Asn119, and Lys122 (**Figure 3**). Detailed interaction energies are summarized in **Table 1**. Compound A (stictic acid) formed two stabilizing hydrogen bonds with Lys115 and Ser81 at distances of 2.95 Å and 2.67 Å, respectively—interactions known to enhance ligand–receptor complex stability [22, 23]. Additional hydrophobic contacts involved residues Phe61, Cys60, His80, Lys62, Gly83, Asn111, and Ala114. Compound B likewise established hydrogen bonding with Lys115 and engaged in hydrophobic interactions with Phe61, Cys60, His80, Lys62, Gly83, Ser81, and Asn111.

**Table 1.** Docking-derived binding energies and interaction characteristics of isolated compounds targeting survivin.

Compound	Binding affinity (kcal/mol)	Electrostatic contribution (kcal/mol)	Predicted Ki (μM)	Hydrogen-bonding atoms (ligand)	Interacting amino acid(s)	Receptor atom(s)	H-bond length (Å)	Key hydrophobic contacts
A*	-5.69	-0.16	67.32	OAN*, OAS*	Ser81, Lys115	OG**, NZ**	2.95, 2.67	His80, Cys60, Lys62, Phe61, Gly83, Asn111, Ala114
B*	-6.72	-2.73	11.90	OAS	Lys115	NZ	2.52	His80, Cys60, Ser81, Lys62, Gly83, Phe61, Asn111

\* The isolated compounds from *Diploschistes ocellatus* include Compound A (stictic acid) and Compound B (2-(7'-hydroxy-3,5,6,8-tetramethyl-9-oxooxonan-2-yl) propanoic acid). Atom types are indicated by the names of the atoms.

**Table 2.** presents the cytotoxic effects of various fractions from *Diploschistes ocellatus* on breast cancer cell lines.

Extract / Fraction	MDA-MB-231 Cells (μg/mL)	T-47D Cells (μg/mL)	MCF-7 Cells (μg/mL)
Water extract	>500	>500	>500
Chloroform extract	166.46 ± 0.056	206.77 ± 0.038	164.10 ± 0.210
Acetone extract	144.36 ± 0.011	81.20 ± 0.064	80.87 ± 0.593
Ethyl acetate extract	114.41 ± 0.016	102.88 ± 0.015	81.23 ± 0.518
Etoposide (reference drug)	19.94 ± 0.006	23.34 ± 0.096	18.53 ± 0.239
Methanolic extract	175.37 ± 0.006	161.63 ± 0.018	213.38 ± 0.462

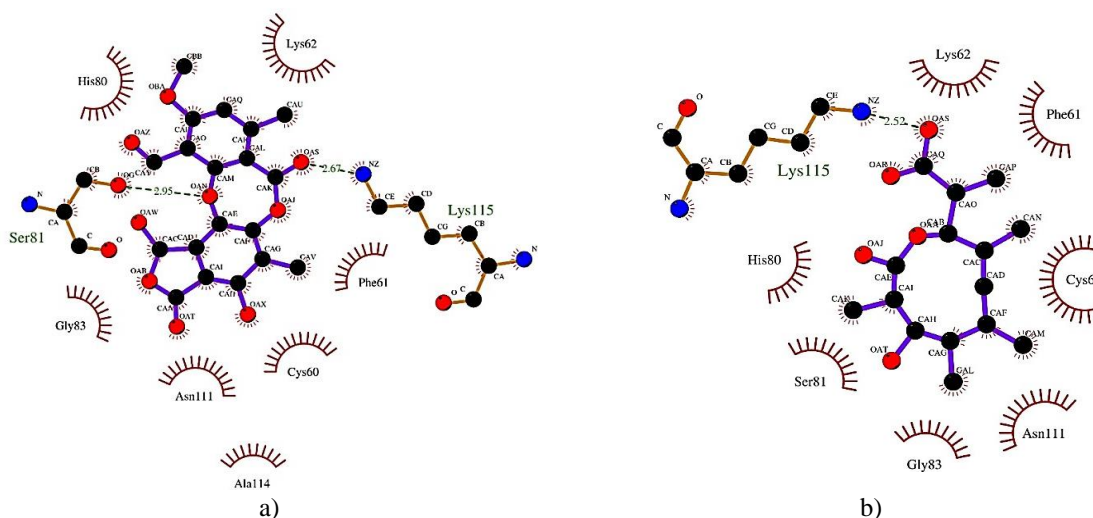


**Figure 3.** illustrates the schematic interactions from the optimal docking poses generated by AutoDock and visualized using LigPlot for survivin with Compound A (stictic acid) and Compound B (2-(7'-hydroxy-3,5,6,8-tetramethyl-9-oxooxonan-2-yl) propanoic acid) from *Diploschistes ocellatus*. Hydrogen bonds are depicted in green, while hydrophobic interactions are represented by brown arcs.

The electrostatic contribution for Compound B was measured at -2.73 kcal/mol, suggesting a favorable protein-ligand interaction. The overall binding free energy for Compound B with survivin was -6.72 kcal/mol, which is considered favorable. Both compounds established hydrogen bonds with the Lys115 residue (**Figures 3a and 3b**).

## Conclusion

This study evaluated the cytotoxic effects of various fractions from *Diploschistes ocellatus* on three human breast cancer cell lines (MCF-7, T-47D, and MDA-MB-231). The acetone fraction exhibited the strongest cytotoxicity, whereas the aqueous fraction displayed no activity. Phytochemical investigation of the acetone fraction identified

stictic acid and 2-(7'-hydroxy-3',5',6',8'-tetramethyl-9'-oxooxonan-2'-yl) propanoic acid as the key compounds likely responsible for the observed cytotoxic effects. Molecular docking simulations targeting survivin inhibition demonstrated favorable interactions between these compounds and survivin residues. These findings suggest that the compounds may modulate apoptosis and warrant further consideration as potential candidates in anticancer therapy.

**Acknowledgments:** None

**Conflict of Interest:** None

**Financial Support:** None

**Ethics Statement:** None

## References

1. Tripathi M, Joshi Y. What are lichenized fungi? In: Endolichenic fungi: present and future trends. Uttarakhand: Springer; 2019.
2. Zambare VP, Christopher LP. Biopharmaceutical potential of lichens. *Pharm Biol.* 2012;50(6):778–98.
3. Gharshi A. Al-Shameel fi al-sinaat al-tibbiah. Tehran: Iran University of Medical Sciences; 2008.
4. Bhattacharyya S, Deep PR, Singh S, Nayak B. Lichen secondary metabolites and its biological activity. *Am J Pharm Tech Res.* 2016;6(6):1–17.
5. Luzina OA, Salakhutdinov NF. Usnic acid and its derivatives for pharmaceutical use: a patent review (2000–2017). *Expert Opin Ther Pat.* 2018;28(6):477–91.
6. Solárová Z, Liskova A, Samec M, Kubatka P, Büsselberg D, Solár P, et al. Anticancer potential of lichens' secondary metabolites. *Biomolecules.* 2020;10(1):87–117.
7. Mendili M, Essghaier B, Seaward M, Khadhri A. In vitro evaluation of lysozyme activity and antimicrobial effect of extracts from four Tunisian lichens. *Arch Microbiol.* 2021;203(4):1461–69.
8. Mendili M, Bannour M, Araújo MEM, Aschi-Smiti S, Seaward MR, Khadhri A, et al. Secondary metabolites and antioxidant capacity of the Tunisian lichen *Diploschistes ocellatus*. *Int J Med Mushrooms.* 2019;21(8):817–23.
9. Neophytou CM, Trougakos IP, Erin N, Papageorgis P. Apoptosis deregulation and the development of cancer multi-drug resistance. *Cancers.* 2021;13(17):4363–88.
10. Shiozaki A, Kataoka K, Fujimura M, Yuki H, Sakai M, Saito S. Survivin inhibits apoptosis in cytotrophoblasts. *Placenta.* 2003;24(1):65–76.
11. Lehner R, Bobak J, Kim NW, Shroyer AL, Shroyer KR. Localization of telomerase hTERT protein and survivin in placenta. *Obstet Gynecol.* 2001;97(6):965–70.
12. Albadari N, Deng S, Chen H, Zhao G, Yue J, Zhang S, et al. Synthesis and biological evaluation of selective survivin inhibitors. *Eur J Med Chem.* 2021;224:113719–81.
13. Jha BN, Shrestha M, Pandey DP, Bhattarai T, Bhattarai HD, Paudel B. Investigation of antioxidant, antimicrobial and toxicity activities of lichens from Nepal. *BMC Complement Altern Med.* 2017;17(1):1–8.
14. Eftekhari M, Ardekani MRS, Amin M, Attar F, Akbarzadeh T, Safavi M, et al. *Oliveria decumbens* essential oil: chemical composition and biological activities. *Iran J Pharm Res.* 2019;18(1):412–21.
15. Eftekhari M, Ardekani MRS, Amin M, Mansourian M, Saeedi M, Akbarzadeh T, et al. Anti-*Helicobacter pylori* compounds from *Oliveria decumbens*. *Iran J Pharm Res.* 2021;20(3):476–89.
16. Morris GM, Huey R, Lindstrom W, Sanner MF, Belew RK, Goodsell DS, et al. AutoDock4 and AutoDockTools4. *J Comput Chem.* 2009;30(16):2785–91.
17. Taheri S, Nazifi M, Mansourian M, Hosseinzadeh L, Shokoohinia Y. Coumarin-quinoline hybrids as apoptotic agents. *Bioorg Chem.* 2019;91:103147–63.
18. Fassihi A, Mahnam K, Moeinifard B, Bahmanziari M, Aliabadi HS, Zarghi A, et al. Novel 1,4-dihydropyridines: synthesis and activity. *Med Chem Res.* 2012;21(10):2749–61.
19. Mahdavi M, Lavi MM, Yekta R, Moosavi MA, Nobarani M, Balalaei S. Spiroquinazolinone derivatives

- in MCF-7 cells. *Chem Biol Interact.* 2016;260:232–42.
20. Chantalat L, Skoufias DA, Kleman JP, Jung B, Dideberg O, Margolis RL. Crystal structure of human survivin. *Mol Cell.* 2000;6(1):183–89.
  21. Javid A, Ahmadian S, Saboury A, Rezaei Zarchi S. Anticancer effect of doxorubicin-loaded nanoparticles. *World Acad Sci Eng Technol.* 2011;50:41–45.
  22. Mishra S, Singh S. Identification of survivin inhibitors: in silico study. *Pharmacogn Mag.* 2017;13(S4):742–48.
  23. Shakeel E, Akhtar S, Khan MKA, Lohani M, Arif JM, Siddiqui MH. Docking analysis of aplysin analogs targeting survivin. *Bioinformation.* 2017;13(9):293–300.
  24. Ismed F, Lohézic-Le Dévéhat F, Rouaud I, Ferron S, Bakhtiar A, Boustie J. NMR reassignment of stictic acid. *Z Naturforsch C.* 2017;72(1–2):55–62.
  25. Fernández Brime S, Llimona X, Lutzoni F, Gaya E. Phylogenetic study of *Diploschistes*. *Taxon.* 2013;62(2):267–80.
  26. Lumbsch HT, Tehler A. Cladistic analysis of *Diploschistes*. *Bryologist.* 1998;101(3):398–403.
  27. Tripathi AH, Negi N, Gahtori R, Kumari A, Joshi P, Tewari LM, et al. Anti-cancer properties of lichen metabolites. *Anti-Cancer Agents Med Chem.* 2022;22(1):115–42.
  28. Pejin B, Iodice C, Bogdanović G, Kojić V, Tešević V. Stictic acid inhibits HT-29 cell growth. *Arab J Chem.* 2017;10(S1):1240–42.